Sensors & Transducers, Vol. 212, Issue 5, May 2017, pp. 70-78

Sensors & Transducers

Published by IFSA Publishing, S. L., 2017
http://www.sensorsportal.com

A Highly Selective Room Temperature NH_3 Gas Sensor based on Nanocrystalline α- Fe_2O_3

Priyanka A. PATIL, Dhanashri G. PATIL, Vinita V. DEO,
and * Lalchand A. PATIL
Nanomaterials Research Laboratory, Department of Physics Pratap College Amalner,
Dist.: Jalgaon, Maharashtra, 425401, India
Tel.: +91-2587-223101/223103, fax: (02587) 223101
E-mail: plalchand_phy_aml@yahoo.co.in

Received: 1 May 2017 /Accepted: 29 May2017 /Published: 31 May 2017

Abstract: Nanocrystalline α-Fe_2O_3 powder was synthesized by simple, inexpensive sol-gel method. The obtained powder was calcined at 700 ^{0}C in air atmosphere for 2 hours. The structural and morphological properties of calcined powder were studied by X-ray diffraction (XRD) and Field Emission Scanning Electron Microscopy (FESEM) respectively. Thermal properties of dried gel were studied by Thermogravimetric Analysis/Differential Scanning Calorimetry (TGA/DSC). The XRD pattern of the powder confirmed the α-Fe_2O_3 (hematite) phase of iron oxide with average crystalline size of 30.87 nm calculated from Scherrer equation. The FESEM images showed uniform wormlike morphology of α-Fe_2O_3 powder. TGA result indicated that α-Fe_2O_3 is thermodynamically stable. Room temperature NH_3 sensing characteristics of α-Fe_2O_3 were studied for various concentration levels (250-2500 ppm) of NH_3 at various humid conditions. The sensor based on α-Fe_2O_3 exhibited good selectivity and excellent sensitivity (S=92) towards 1000 ppm of NH_3 with quick response of 4 sec and fast recovery of 9 sec. Room temperature sensing mechanism is also discussed.

Keywords: α-Fe_2O_3, Sol-gel, NH_3 sensing, Room temperature.

1. Introduction

The huge industrial development all over the world leads to increase in environmental pollution by releasing hazardous gases and vapors in the surrounding. NH_3 plays an important role in all forms of life. It is naturally produced in living organisms. NH_3 is widely used in the production of nitrogenous fertilizers, chemicals and petrochemical industries etc. It is also used as an industrial refrigerant. NH_3 is colorless gas with pungent smell. It is very toxic and can cause burns on the skin, in the eyes, in the respiratory system and in the lungs which can lead permanent blindness and lung diseases [1-4]. Therefore, it is necessary to develop NH_3 sensors with fast response time and low detection limit at room temperature.

Previous research shows NH_3 can be detected by using potentiometric electrode, infrared devices, optical fibers, conducting polymers and metal oxides [5, 6]. Among all these, metal oxide gas sensors are widely used because of their simplicity of production and use, low cost and capability of detecting wide range of toxic gases and vapors under different conditions. Various metal oxide semiconductors such as SnO_2, ZnO, V_2O_5, ITO, WO_3 and TiO_2 are being used as NH_3 sensors [7].

α-Fe_2O_3 (hematite) is one of the promising metal oxides due to its potential applications in many fields such as gas sensors, lithium batteries, catalysis, pigment and magnetic devices [8-12]. It is thermodynamically most stable phase of iron oxides. α-Fe_2O_3 exhibits n-type semiconducting properties with an energy gap of 2.2 eV [13]. Various techniques have been employed for the synthesis of α-Fe_2O_3 nanocrystalline powder such as chemical coprecipitaion, hydrothermal method and sol-gel technique etc. Here sol-gel method is used for synthesis of α-Fe_2O_3 nanocrystalline powder because it is simple and cost effective [8, 14, 15].

Most of the metal oxide NH_3 gas sensors are operated effectively only at higher temperatures (150-400^{0}C), which results in high power consumption. Hence it is necessary to develop gas sensors that would have good results at room temperature [16]. But from available literature it is rare to find unmodified α-Fe_2O_3 as NH_3 sensor at room temperature with excellent sensitivity, good selectivity and quick response and recovery times.

In the present investigation, experiments have been carried out for the fabrication of room temperature NH_3 sensor based on α-Fe_2O_3. The sensing characteristics of α-Fe_2O_3 are reported.

2. Materials and Methods

2.1. Materials

All chemicals were used of analytical grade. Chemicals used for synthesis of α-Fe_2O_3 powder were ferric nitrate (Fe $(NO_3)_3.9H_2O$), ethanol, triethylamine (TEA) and glycerol.

2.2. Synthesis of α-Fe_2O_3 Powder

0.1 M of Fe $(NO_3)_3.9H_2O$ was dissolved in 20 ml ethanol under permanent magnetic stirring at 350-400 rpm. The temperature of the solution was maintained at 60 °C using water bath. After complete dissolution orange colored transparent sol was obtained. Subsequently 6 ml of TEA was added to the solution drop by drop. The color of solution rapidly changed from orange to a reddish brown accompanied by appreciable heat release and the dark brown color gel was set within 30 minutes. After two hours, the gel was completely dried. The dried gel was calcined at 700 °C in air atmosphere for 2 hours to obtain the α-Fe_2O_3 powder.

2.3. Characterization Techniques

The structural property of the synthesized powder was investigated using X-ray diffractometer (Miniflex 600, Rigaku) with CuKα1 radiation (λ= 1.5406 Å). The morphology of powder was studied using field emission scanning electron microscopy (FESEM model S4800 type II, Hitachi High Technologies). Quantitative analysis was carried out using energy dispersive analysis by X-rays (EDAX model Bruker Nano GmbH X Flash Detector 5030) equipped with FESEM. Thermo gravimetric analysis (TGA) of the dried gel (xerogel) was done by STA-6000 (Perkin Elmer) in the temperature range of 50-800 °C under nitrogen atmosphere.

2.4. Fabrication of α-Fe_2O_3 Gas Sensor and Gas Sensing System

2.4.1. Fabrication of α-Fe_2O_3 Gas Sensor

α-Fe_2O_3 gas sensor was fabricated by screen printing technique. The thixotropic paste of α-Fe_2O_3 powder was prepared by mixing the fine powder with a temporary organic binder (1-acetoxy 2-butoxy ethane +2-butoxyethanol + terpineole + ethyl cellulose). The ratio of inorganic part to organic part was kept 75:25 in formulating the paste. This paste was screen printed on the glass substrates in desired patterns. Thus obtained thick films were fired at 500 ^{0}C for 30 minutes. The obtained thick films were termed as α-Fe_2O_3 sensor.

2.4.2. Gas Sensing Setup

To study the changes in electrical properties of the gas sensor, electrical contacts were made on film surface using copper wire and silver paste. The gas sensing set-up is as shown in Fig. 1.

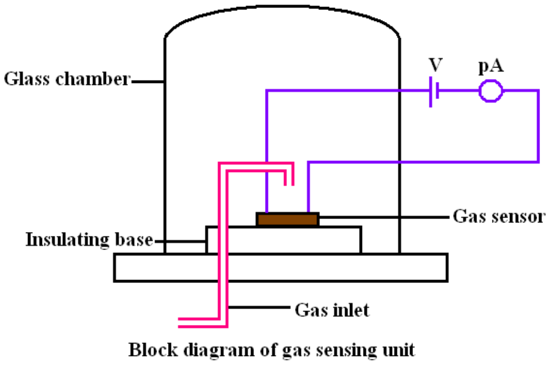

Fig. 1. Block diagram of gas sensing system.

The gas sensor was kept inside the glass chamber. A constant voltage (2V) was applied to the electrodes of α-Fe_2O_3 sensor and the current flowing through it was measured with picoammeter. The known volume of gas was injected into the glass chamber. The current before exposure of target gas (I_a) and the current on exposure of target gas (I_g) was measured. The performance of gas sensor was expressed in terms of gas response (S) and is defined as the ratio of change in conductance of the gas sensor on the exposure of target gas to the conductance before exposure of target gas [17]. Gas sensing study is carried out at room temperature (R_T) which is about 35 °C.

$$S = \frac{I_g}{I_a} \tag{1}$$

2.4.3. Gas Concentration Calculation

The desired gas concentration of the gas was calculated by using equation (2) [18]

$$V = \frac{Cppm \times Va \times M}{24.5 \times 10^9 \times D}, \tag{2}$$

where V is the required liquid volume, C_{ppm} is gas concentration in ppm, V_a is volume of test chamber, M is molecular weight of liquid, D is the density of liquid.

All units were measured in mililitres, cubic centimeters and grams.

The appropriate volume of liquor NH_3 calculated from (2) was taken in conical flask by the aid of micro syringe. The flask was slowly heated on magnetic stirrer. NH_3 liquid gets converted into NH_3 gas. As prepared NH_3 gas was observed to be wet as tested by pH paper. The wet NH_3 was passed through calcium oxide (CaO) to reduce the water vapors and get dry NH_3. The detailed procedure of preparing and drying NH_3 is given in supplementary information.

3. Results and Discussion

3.1. XRD Study

The XRD pattern of α- Fe_2O_3 thick film is shown in Fig. 2.

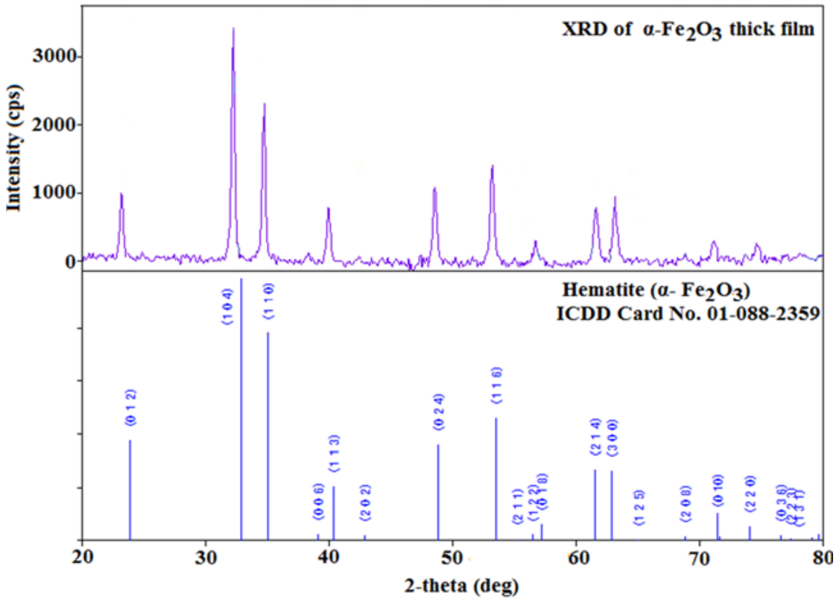

Fig. 2. XRD pattern of α- Fe_2O_3 thick film.

The strong diffraction peaks were observed to be hematite (α- Fe_2O_3) phase of iron oxide (ICDD Card No. 01-088-2359). From Fig. 2 it can be seen that there is significant difference in the peak position between the reference data and presented XRD pattern. This peak shifting occurs due to specimen displacement error. The specimen displacement error is due to the misalignment of the sample [19].

The average crystalline size of the prepared α-Fe_2O_3 powder was calculated by Scherrer equation (3).

$$D = \frac{0.9\lambda}{\beta cos\theta} \tag{3}$$

The average crystalline size of α-Fe_2O_3 nanocrystalline powder from Scherrer equation is found to be 30.87 nm.

3.2. FESEM Study

Fig. 3 shows field emission scanning electron microscopic (FESEM) images of α- Fe_2O_3 thick film. Fig. 3 indicates wormlike morphology of α- Fe_2O_3 thick film [20].

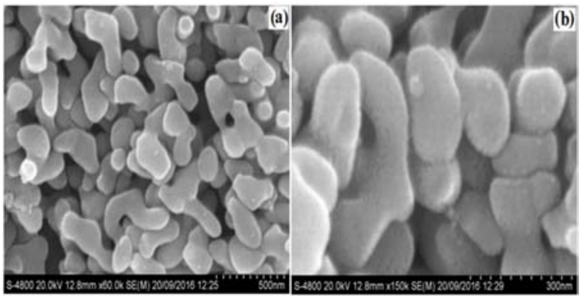

Fig. 3. FESEM images of α- thick film.

3.3. TGA/DSC Study

Fig. 4 shows the TG and DSC curves of xerogel. The weight loss of 4.94 % below 120 °C resulted from the evaporation of the adsorbed water. The weight loss of 44.02 % from 120°C-350 °C with sharp exothermic peak at 141°C can be ascribed to the decomposition of the residual organic molecules. The small exothermic peak at 355 °C in DSC curve correspondence to the transformation of γ-Fe_2O_3 to α-Fe_2O_3 phase [21, 22]. Within the temperature range of 355 °C- 800 °C the weight loss is only 1.3 % which indicates that the α-Fe_2O_3 is thermodynamically stable above 355 °C.

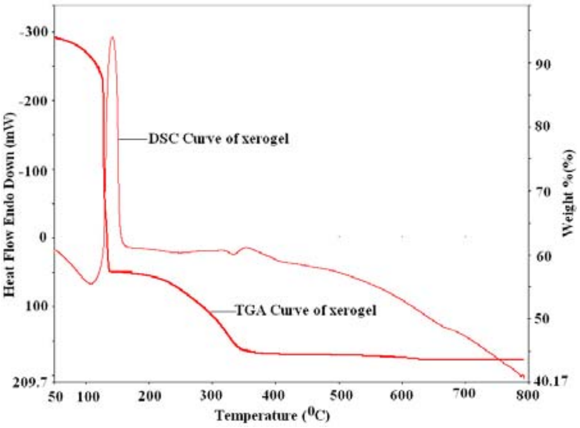

Fig. 4. TGA/DSC curve of xerogel.

3.4. Gas Sensing Study

Fig. 5 shows the room temperature I-V characteristics of the α-Fe_2O_3 thick film in the voltage range -25 V to +25 V. The obtained I-V curve shows the ohmic contacts between the copper wire and the thick film.

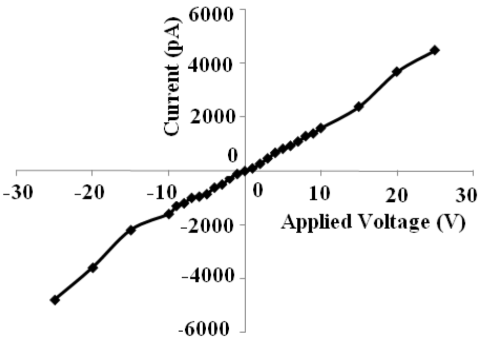

Fig. 5. I-V characteristics of the α-Fe_2O_3 thick film.

3.4.1. Selectivity

Selectivity is an important parameter of gas sensors. Selectivity is defined as the ability of gas sensor to identify a specific gas in presence of other gases [23]. Fig. 6 shows the room temperature response of α- Fe_2O_3 to 1000 ppm of different gases such as NH_3, methanol, ethanol, isopropanol and acetone.

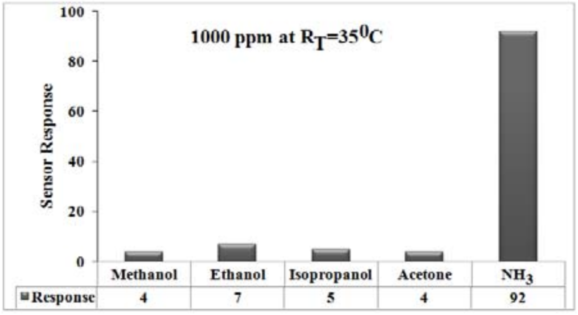

Fig. 6. Selectivity of α-Fe_2O_3 sensor.

It can be seen from Fig. 6 that α- Fe_2O_3 sensor is highly selective to NH_3 at room temperature. Selectivity to NH_3 can be quantified in terms of selectivity coefficient (K). The selectivity coefficient (K) is defined in equation (4)

$$K = \frac{S_{NH3}}{S_{gas}}, \quad (4)$$

where S_{NH3} is the response of sensor to NH_3, S_{gas} is the response of sensor to other gas.

Generally selectivity coefficient should be greater than 5 [13, 24]. Selectivity coefficients were 23 to methanol, 13 to ethanol, 18 to isopropanol and 23 to acetone.

3.4.2. Effect of Temperature

Though the aim of this study was to develop room temperature NH_3 sensor, we also tested the sensor to 1000 ppm NH_3 at different temperatures such as 35, 45, 55 65, 100 and 150 °C to study the effect of temperature on sensitivity of different gases. The obtained responses of sensor are shown in Fig. 7.

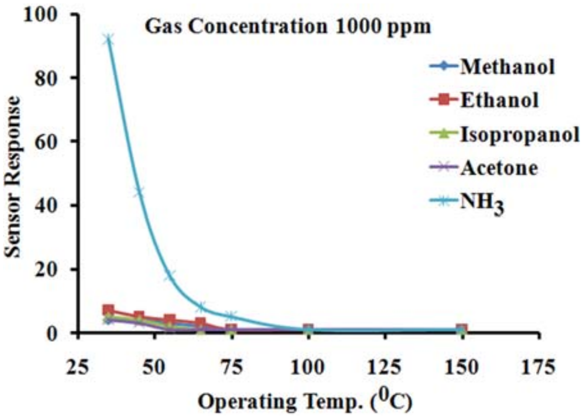

Fig. 7. Sensor response as a function of operating temperature.

It is clear from Fig. 7 that the sensor response significantly decreases with increase in operating temperatures.

As the temperature of sensor surface increases, the surface electrolyte layer is evaporated and there is no possibility of ionic conduction resulting in no response towards NH_3 at 100 and 150 °C. In this case humidity plays an important role in the sensor response. As the temperature increases, humidity decreases resulting in no adsorption of water molecules on sensor surface and hence no sensor response towards NH_3 [25].

3.4.3. Effect of Humidity

Relative humidity (RH %) is defined as the ratio of the amount of water vapor in the air at specific temperature to the maximum amount that the air could hold at that temperature. It is expressed in percentage (%). Relative humidity (RH %) is an important parameter in determining the response of metal oxide gas sensors and especially in case of gas sensors operating at room temperature. Hence the effect of RH on response to NH_3 has been studied at different humid conditions such as 11 %, 27 %, 37 %, 47 %, 57 %, 67 %, 78 % and 87 % of RH. Fig. 8a shows the effect of humidity on sensor response of different gases.

Fig. 8b shows the variation in sensor response with relative humidity when exposed to 1000 ppm of NH_3.

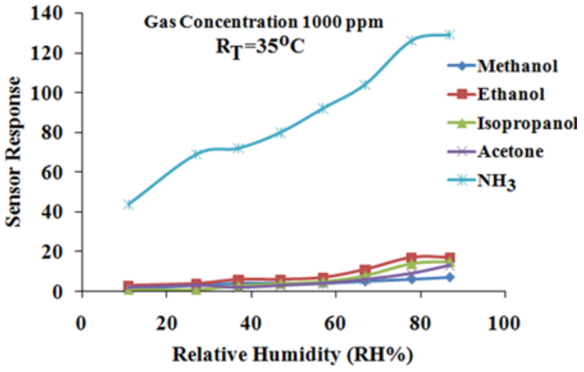

Fig. 8a. Effect of humidity on sensor response of different gases.

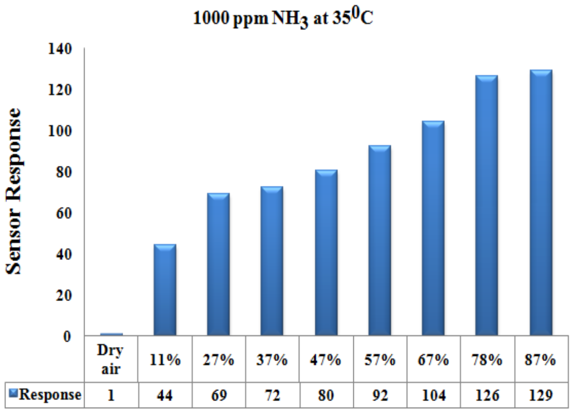

Fig. 8b. Effect of humidity on NH3 sensor response.

Under the humid conditions the response of sensor towards 1000 ppm of NH_3 was found to be increased. This might be due to the increase in number of adsorbed water molecules on sensor surface and ultimately change in sensing properties of sensor surface [26, 27]. When the NH_3 sensing characteristics were carried out in dry air, no response to NH_3 was detected due to the absence of thin layer of adsorbed water on sensor surface. If there will be no humidity there will be no response hence humidity plays a significant role in sensing at room temperature.

3.4.4. Effect of Gas Concentration

The α-Fe_2O_3 sensor response as a function of gas concentrations of different test gases is as shown in Fig. 9a and Fig. 9b.

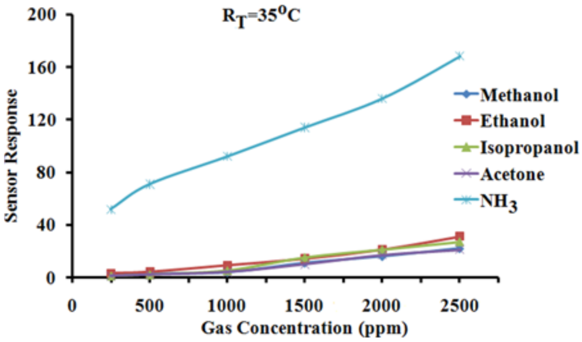

Fig. 9a. Sensor response to different concentrations of gases.

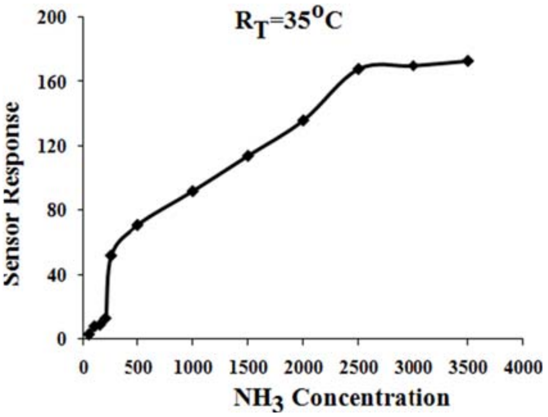

Fig. 9b. Sensor response to different concentrations of NH_3.

It can be seen from Fig. 9a that α-Fe_2O_3 sensor response exhibits a nearly linear increase with increasing concentration of different gases. The α-Fe_2O_3 sensor response increased linearly with NH_3 concentration from 250 ppm to 2500 ppm and saturates beyond it as shown in Fig. 9b. Even after the further increase of NH_3 concentration there was no significant increase in response. The sensor response saturated above 2500 ppm because of formation of multilayer of NH_3 over the sensor surface which restricted the further interaction of NH_3 molecules with adsorbed water molecules. Hence the sensor response reached at saturation above 2500 ppm. At lower concentration 250 ppm, sensor response was found to be 52. Further decrease in NH_3 concentration (<250 ppm) does not produce considerable response. This might be due to less interaction of NH_3 molecules with adsorbed water molecules. Hence, the detection limit for NH_3 at room temperature was determined to be in the range of 250-2500 ppm [28].

3.4.6. Response and Recovery Time

The response time (T_{Res}) is defined as the time taken by the sensor to reach maximum steady state current change on the exposure of target gas with the surface of the sensor. The recovery time (T_{Rec}) is defined as the time required for the sensor current to reach the base line after the removal of the target gas [29].

Fig. 10 shows the steady state response properties of α- Fe_2O_3 gas sensor operated at room temperature under 1000 ppm of NH_3. The steady state response properties were measured by introducing constant flow of 1000 ppm of NH_3 for 25 sec in glass chamber. The baseline currents before exposure of NH_3 were measured. The current through sensor increases on exposure of NH_3 and attains to maximum current value in 4 sec and remains in steady state till the exposure of NH_3 is on. The current through sensor falls to the baseline current in 9 sec once the exposure of NH_3 was off.

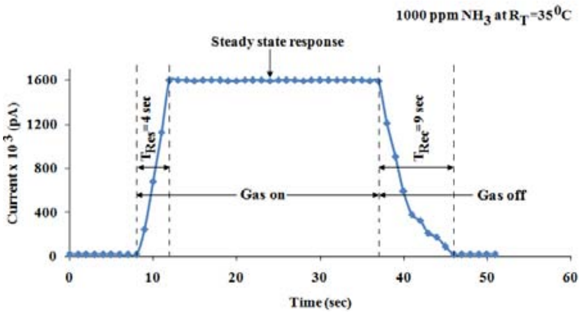

Fig. 10. Steady state response properties of α- Fe_2O_3 sensor.

It could be seen from Fig. 10 that the α- Fe_2O_3 gas sensor has fast response time of 4 sec and quick recovery time of 9 sec. Adsorption and desorption of NH_3 molecules occur rapidly because of large surface area of α- Fe_2O_3 gas sensor and lower molecular weight of NH_3 molecule which results in fast response and quick recovery of sensor [1].

The comparison of present α- Fe_2O_3 sensor with other reported sensors for NH_3 is summarized in Table 1.

Table 1. Comparison of sensor responses toward NH_3 of various gas sensors.

Sr. No	Material	Operating Temp. (°C)	Gas concentration (ppm)	Sensor Response	T_{Res} (S)	T_{Rec} (S)	Reference
1	α-Fe_2O_3	RT	1000	92	4	9	Present work
2	Sr-SnO2	RT	2000	54.23%	6	-	28
3	PANI/SnO_2	RT	100	29	-	-	29
4	QDS/TiO_2	RT	100	17.49	-	-	30
5	SnO_2-SnS_2	RT	500	2.2	11	-	31
6	ZnO	RT	400	1.15	240	290	32

Table 1 shows that the response towards NH_3 of present α- Fe_2O_3 sensor is higher with fast response and quick recovery time than other reported sensors.

3.4.7. Gas Sensing Mechanism

Metal oxide semiconductor exhibits two kinds of gas sensing mechanisms (i) dissociative gas sensing mechanism which takes place at low temperature (T_{opt} < 100 °C), (ii) combustive gas sensing mechanism which takes place at high temperatures (T_{opt} > 100 °C).

Here we discuss the dissociative gas sensing mechanism at room temperature. At room temperature, metal oxide semiconductor surface is covered with thin layer of adsorbed humidity. In such a condition direct gas sensing mechanism is not possible. At room temperature, gas response in humid atmosphere is controlled by the pH of thin layer of adsorbed water. This electrolytic layer with metal oxide semiconductor surface acts as pH sensor. The pH of the surface electrolyte changes with the interaction of analyte gas with the surface electrolyte. This pH change in surface electrolyte changes the ionic and electronic conductivities of metal oxide semiconductor surface resulting in detectable electrical output signal.

3.4.7.1. Before Exposure of NH_3

Water undergoes dissociative adsorption on metal oxide surface as:

$$H_2O \leftrightarrow H^+ + OH^-$$

Chemisorption of water molecules is possible at low humidity level while physisorption is observed at higher humidity levels. At low humidity level electronic conduction is dominant. Fig. 11 and equation (5) correspond to case of water molecule interacting with metal oxide, two Fe-OH dipoles are formed from dissociated hydroxyl ions and by combination of hydrogen ion and lattice oxygen. Two free electrons are produced from each oxygen vacancy (V_o^{2+}) in the lattice during formation of Fe-OH bond [26, 35-37].

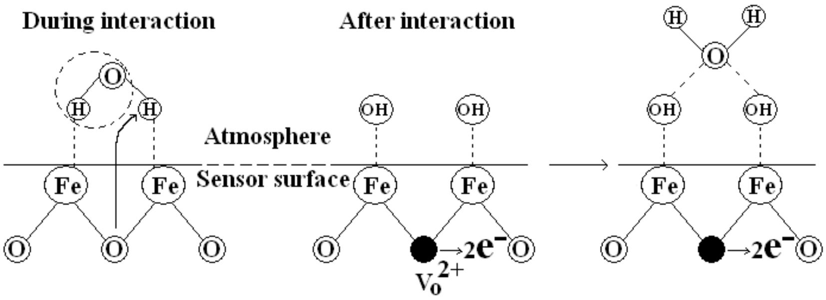

Fig. 11. Mechanism of humidity adsorption on α-Fe₂O₃ sensor surface.

$$H_2O + 2(Fe_{Fe} + O_o) \leftrightarrow 2\left(Fe_{Fe}^{\delta+} - OH^{\delta-}\right) + V_O^{2+} + 2e^- \qquad (5)$$

3.4.7.2. After Exposure of NH_3

At room temperature layer of water molecules adsorbed on the α-Fe_2O_3 sensor surface. This adsorbed water layer acts as liquid electrolyte. NH_3 is basic molecule and it has lone pair of electrons. NH_3 can easily dissociate electrolytically in water.

When NH_3 is exposed on α-Fe_2O_3 sensor surface, it penetrates into the liquid electrolyte followed by the electrolytic dissociation of NH_3 molecule in NH_4^+ and OH^- ions according to the equation (6). The dissociation of NH_3 molecules changes the ionic concentration inside the electrolytic layer by increasing the ionic conductivity and change in pH value.

$$NH_{3(gas)} + H_2O_{(aq.)} \leftrightarrow NH_{4(aq.)}^{+} + OH_{(aq.)}^{-} \qquad (6)$$

After every such reaction, one electron releases and conductivity of the α-Fe_2O_3 sensor increases on exposure of NH_3 gas. Interaction of NH_3 with α-Fe_2O_3 sensor surface through liquid electrolyte is as shown in Fig. 12. At room temperature NH_3 sensing may be due to the change in ionic and electronic conductivities. In the present study electronic conduction is dominant over ionic conduction because the humidity level is low in the surrounding [38-41].

3.4.8. Stability

Stability is important parameter for room temperature gas sensors. Stability is defined as the ability of the sensor to give reproducible results for certain period of time. The stability and reproducibility of α- Fe_2O_3 sensor were studied for 1000 ppm of NH_3 at room temperature over the period of 30 days. Fig. 13 showed obtained response and indicates that **α**- Fe_2O_3 sensor is stable for 1000 ppm of NH_3 over a period of 30 days. The sensing studies were repeated to the α-Fe_2O_3 sensor stored over the period of 4 months.

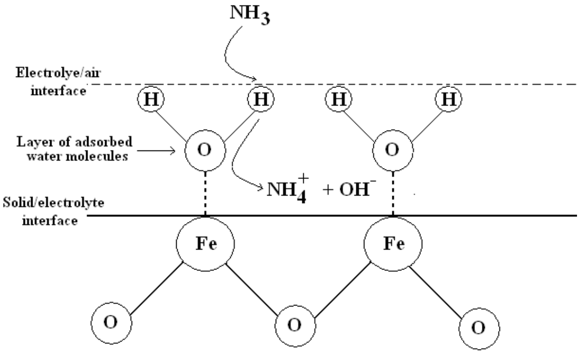

Fig. 12. Interaction of NH_3 with α-Fe_2O_3 sensor surface.

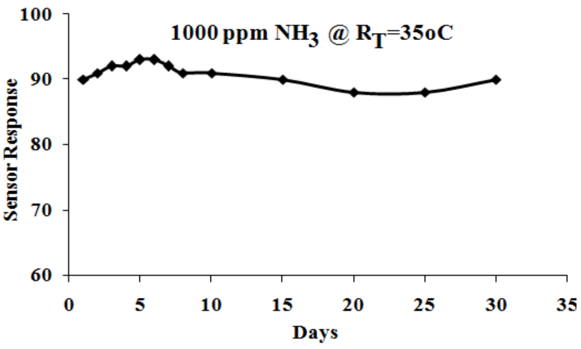

Fig. 13. Stability of α- Fe_2O_3 sensor towards 1000 ppm of NH_3.

4. Conclusions

In the summery, we have synthesized nanocrystalline α- Fe_2O_3 simple sol gel method. The structural, morphological and thermal properties of α-Fe_2O_3 powder were studied by different analytical techniques. Sensing characteristics of α- Fe_2O_3 sensor were examined towards the various gases at room temperature under different humid conditions. α-Fe_2O_3 sensor was found to be highly selective and showed excellent response towards NH_3 at room temperature under humid conditions. In dry air, no response to NH_3 was detected. It has been demonstrated that humidity plays a key role in the NH_3 sensing at room temperature. The considerable linear change in sensor response was observed over the range of 250-2500 ppm. The lower NH_3 detection limit was found to be 250 ppm. The α-Fe_2O_3 sensor exhibited excellent sensitivity (S=92) towards 1000 ppm of NH_3 with quick response of 4 sec and fast recovery of 9 sec. The α-Fe_2O_3 sensor showed good stability and reproducibility.

Acknowledgements

Authors are heartily thankful to Head, INSPIRE Program, Department of Science & Technology, New Delhi. The authors also would like to thank Head of Physics Department and Principal Pratap College Amalner, Dist: Jalgaon, Maharashtra for providing laboratory facilities.

References

[1]. C. Balamurugam, D. W. Lee, A selective NH_3 gas sensor based on mesoporous p-type NiV_2O_6 semiconducting nanorods synthesized using solution method, *Sensors Actuators B: Chemical,* Vol. 192, 2014, pp. 414-422.

[2]. V. Balouria, A. Kumar, S. Samanta, A. Singh, A. K. Debnath, A. Mahajan, R. K. Bedi, D. K. Aswal, S. K. Gupta. Nano-crystalline Fe_2O_3 thin films for ppm level detection of H_2S, *Sensors Actuators B: Chemical,* Vol. 181, 2013, pp. 471-478.

[3]. P. Dhivya, A. K. Prasad, M. Shridharan. Nanostructured TiO_2 films: Enhanced NH_3 detection at room temperature, *Ceramics International*, Vol. 40, Issue 1, 2014, pp. 409-415.

[4]. R. Pandeeswari, B. G. Jeyaprakash, High sensing response of β-Ga_2O_3 thin film towards ammonia vapours: Influencing factors at room temperature, *Sensors Actuators B: Chemical,* Vol. 195, 2014, pp. 206-214.

[5]. S. K. Dhawan, D. Kumar, M. K. Ram, S. Chandra, D. C. Trivedi, Application of conducting polyaniline as sensor material for ammonia, *Sensors Actuators B: Chemical*, Vol. 40, 1997, pp. 99-103.

[6]. C. Malins, A. Doyle, B. D. MacCraith, F. Kvasnik, M. Landl, P. Simon, L. Kalvoda, R. Lukas, K. Pufler, I. Babusik. Personal ammonia sensor for industrial environments, *Journal of Environment and Monitoring*,, Vol. 4, Issue 5, 1999, pp. 417-422.

[7]. B. Timmer, W. Olthuis, A. V. D. Berg, Ammonia sensors and their applications – a review, *Sensors Actuators B: Chemical,* Vol. 107, 2005, pp. 666-677.

[8]. P. Sun, W. Eang, Y. Liu, Y. Sun, J. Ma, G. Lu, Hydrothermal synthesis of 3D urchin-like α-Fe_2O_3 nanostructure for gas sensor, *Sensors Actuators B: Chemical,* Vol. 173, 2012, pp. 52-57.

[9]. P. Zhang, Z. G. Ping, H. K. Liu. Submicron-sized cube-like α-Fe_2O_3 agglomerates as an anode material for Li-ion batteries, *Electrochemical Acta*, Vol. 55, Issue 28, 2010, pp. 8521-8526.

[10]. L. Li, Y. Chu, Y. Liu, L. Dong, Template-Free Synthesis and Photocatalytic Properties of Novel Fe_2O_3 Hollow Spheres, *Journal of Physics and Chemistry C*, Vol. 111, Issue 5, 2007, pp. 2123-2127.

[11]. F. Bodily, A. M. Ferrari, C. Leonel, T. Manfredini, Hydrothermal Preparation and Characterization of Nanocrystalline Powder of β-Indium Sulfide, *Materials Research Bulletin*, Vol. 33, Issue 5, 1998, pp. 723-729.

[12]. J. Ma, J. Lian, X. Duan, X. Liu, W. Zheng, α-Fe_2O_3: Hydrothermal synthesis, magnetic and electrochemical properties, *Journal of Physics and Chemistry C*, Vol. 114, Issue 24, 2010, pp. 10671–10676.

[13]. D. Patil, V. Patil, P. Patil, Highly sensitive and selective LPG sensor based on α-Fe_2O_3 nanorods, *Sensors Actuators B: Chemical,* Vol. 152, 2011, pp. 299-306.

[14]. L. Duraes, B. F. O. Costab, J. Vasquesa, J. Camposc, A. Portugala, Phase investigation of as-prepared iron oxide/hydroxide produced by sol - gel synthesis, *Materials Letters,* Vol. 59, Issue 7, 2005, pp. 859-863.

[15]. L. Duraes, A. Moutinho, I. J Seabra, B. F. O. Costa, H. C. de Sousa, A. Portugal, Characterization of iron (III) oxide/hydroxide nanostructured materials produced by sol - gel technology based on the Fe $(NO_3)_3 \cdot 9H_2O$ - C_2H_5OH - CH_3CHCH_2O system, *Materials Chemistry and Physics,* Vol. 130, Issue 1-2, 2011, pp. 548-560.

[16]. N. V. Hieu, N. Q. Dung, P. D. Tam, T. Trung, N. D. Chien, Thin film polypyrrole/SWCNTs nanocomposites-based NH_3 sensor operated at room temperature, *Sensors Actuators B: Chemical*, Vol. 140, 2009, pp. 500-507.

[17]. V. V. Deo, D. M. Patil, L. A. Patil, M. P. Kaushik, Ultrasonically sprayed nanostructured $CdSnO_3$ thin films for the detection of VOC's, *Sensors Actuators B: Chemical*, Vol. 196, 2014, pp. 489-496.

[18]. K. Arshak, I. Gaidan, NiO / Fe_2O_3 polymer thick films as room temperature gas sensors, *Thin Solid Films*, Vol. 495, Issue 1-2, 2006, pp. 286-291.

[19]. B. D. Cullity, Elements of X-ray Diffraction, 2nd edition, *Addison-Wesley,* Reading, MA, 1978.

[20]. L. Wan, K. Shi, X. Tian, H. Fu, Facile synthesis of iron oxide with wormlike morphology and their application in water treatment, *Solid State Chemistry*, Vol. 181, Issue 4, 2008, pp. 735-740.

[21]. J. S. Xu, Y. J. Zhu, Monodisperse Fe_3O_4 and γ-Fe_2O_3 magnetic mesoporous microspheres as anode materials for lithium-ion batteries, *ACS Applied Materials Interfaces*, Vol. 4, Issue 9, 2012, pp. 4752−4757.

[22]. E, Darezereshki, One-step synthesis of hematite (α-Fe_2O_3) nano-particles by direct thermal-decomposition of maghemite, *Materials Letters*, Vol. 65, Issue 4, 2011, pp. 642–645.

[23]. L. A. Patil, A. R. Bari, M. D. Shinde, Vinita Deo, M. P. Kaushik, Detection of dimethyl methyl phosphonate -a simulant of sarin: The highly toxic chemical warfare using platinum activated nanocrystalline ZnO thick films, *Sensors Actuators B: Chemical*, Vol. 161, 2012, pp. 372– 380.

[24]. X. Zhao, Z. Li, X. Lou, M. Li, N. Zhang. Room-temperature chlorine gas sensor based on $CdSnO_3$ synthesized by hydrothermal process, *Journal of Advanced Ceramics*, Vol. 2, Issue 1, 2013, pp. 31-36.

[25]. A. Helwig, G. Müller, G. Sberveglieri, M. Eickhoff, On the low-temperature response of semiconductor gas sensors, *Journal of Sensors*, 2009, pp. 1-17, Article ID 620720.

[26]. P. Shankar, J. B. B Rayappan, Gas sensing mechanism of metal oxides: The role of ambient atmosphere, type of semiconductor and gases - A review, *Science Letters Journal*, Vol. 126, Issue 4, 2015, pp. 1-16.

[27]. G. K. Mani, J. B. B. Rayappan, A highly selective room temperature ammonia sensor using spray deposited zinc oxide thin film, Sensors *Actuators B: Chemical,* Vol. 183, 2013, pp. 459-456.

[28]. S. T. Navale, D. K. Bandgar, S. R. Nalage, G. D. Khuspe, M. A. Chougule, Y. D. Kolekar, S. Sen, V. B. Patil. Synthesis of Fe_2O_3 nanoparticles for nitrogen dioxide gas sensing applications, *Ceramics International*, Vol. 39, Issue 6, 2013, pp. 6453-6460.

[29]. L. A. Patil, M. D. Shinde, A. R. Bari, V. V. Deo, Highly sensitive ethanol sensors based on nanocrystalline SnO_2 thin films, *Current Applied Physics*, Vol. 10, Issue 5, 2010, pp. 1249-1254.

[30]. S. Xu, K. Kan, Y. Yang, C. Jiang, J. Gao, L. Jing, P. Shen, L. Li, K. Li, Enhanced NH_3 gas sensing performance based on electrospun alkaline-earth metals composited SnO_2 nanofibers, *Journal of Alloys and Compounds*, Vol. 618, 2015, pp. 240-247.

[31]. S. Bai, Y. Tian, M. Cui, J. Sun, Y. Tian, R. Luo, A. Chen, D. Li, Polyaniline@SnO_2 heterojunction loading on flexible PET thin film for detection of NH_3 at room temperature, *Sensors Actuators B: Chemical*, Vol. 226, 2016, pp. 540–547.

[32]. Y. Liu, L. Wang, H. Wang, M. Xiong, T. Yang, G. S. Zakharova, Highly sensitive and selective ammonia gas sensors based on PbS quantum dots/TiO_2 nanotube arrays at room temperature, *Sensors Actuators B: Chemical*, Vol. 236, 2016, pp. 529–536.

[33]. K. Xu, N. Li, D. Zeng, S. Q. Tian, S. S. Zhang, D. Hu, C. Xie, Interface bonds determined gas-sensing of sno_2–sns_2 hybrids to ammonia at room temperature, *ACS Applied Materials Interfaces*, Vol. 7, Issue 21, 2015, pp. 11359–11368.

[34]. A. Kshirsagar, A. B. Joshi, A. Joshi, D. K. Avasthi, T. M. Bhave, S. A. Gangal, Comparative study of irradiated and annealed ZnO thin films for room temperature ammonia gas sensing, IEEE *Sensors Conference 2007*, Atlanta, GA, USA, 28-31 October 2007, pp. 162-165.

[35]. Z. Chen, C. Lu, Humidity Sensors: A Review of Materials and Mechanisms, *Sensors Letters*, Vol. 3, Issue 4, 2005, pp. 274-295.

[36]. Y. C. Yeh, T. Y. Tseng, D. A. Chang, Electrical properties of TiO_2-$K_2Ti_6O_{13}$ porous ceramic humidity sensor, *Journal of American Ceramic Society*, Vol. 73, Issue 7, 1990, pp. 1992-1998.

[37]. Y. Shimizu, M. Shimabukuro, H. Arai, T. Seiyama, Humidity-sensitive characteristics of La^{3+}-doped and undoped SrSnO3, *Journal of Electrochemical Society*, Vol. 136, Issue 4, 1989, pp. 1206-1210.

[38]. A. Helwig, G. Müller, O. Weidemann, A. Härtl, J. A. Garrido, M. Eickhoff, Gas sensing interactions at hydrogenated diamond surfaces, *IEEE Sensors Journal*, Vol. 7, Issue 9, 2007, pp. 1349–1353.

[39]. A. Helwig, G. Müller, G. Sberveglieri, G. Faglia, Gas sensing properties of hydrogenated amorphous silicon films, *IEEE Sensors Journal*, Vol. 7, Issue 11, 2007, pp. 1506–1512.

[40]. A. Helwig, G. Muller, M. Eickhoff, G. Sberveglieri, Dissociative gas sensing at metal oxide surfaces, *IEEE Sensors Journal*, Vol. 7, Issue 12, 2007, pp. 1675–1679.

[41]. S. Beer, A. Helwig, G. Muller, J. Garrido, M. Stutzmann. Water adsorbate mediated accumulation gas sensing at hydrogenated diamond surfaces, *Sensors Actuators B: Chemical*, Vol. 181, 2013, pp. 894– 903.
